Ecological Indicators 150 (2023) 110219

Contents lists available at ScienceDirect

Ecological Indicators

journal homepage: www.elsevier.com/locate/ecolind

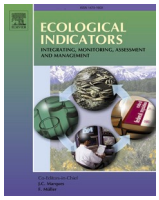

Original Articles

Potential distribution of two economic laver species-*Neoporphyra haitanensis* and *Neopyropia yezoensis* under climate change based on MaxEnt prediction and phylogeographic profiling

Wenyuan Zhou [a,b], Baoxian Li [b], Hui Xu [a,b], Zhourui Liang [b,c], Xiaoping Lu [b], Lien Yang [d], Wenjun Wang [b,c,*]

[a] *Zhejiang Ocean University, Zhoushan, China*
[b] *Key Laboratory of Sustainable Development of Marine Fisheries, Ministry of Agriculture and Rural Affairs, Yellow Sea Fisheries Research Institute, Chinese Academy of Fishery Sciences, Qingdao, China*
[c] *Laboratory for Marine Fisheries Science and Food Production Processes, Laoshan Laboratory, Qingdao, China*
[d] *Jiangsu Marine Fisheries Research Institute, Nantong, China*

ARTICLE INFO

Keywords:
Chloroplast *rbc*L sequence
Distribution centroid
Global warming
Haplotype
Genetic diversity
Species distribution model

ABSTRACT

Climate change is altering geographic and phylogeographic distribution of macroalgae, laying great impacts on their conservation and sustainable utilization. The potential distribution of two dominant cultured seaweeds-*Neoporphyra haitanensis* and *Neopyropia yezoensis* was predicted under present and three representative concentration pathways (RCP 2.6, 4.5, 8.5) for 2050 s using the maximum entropy model (MaxEnt). The area under the receiver operating characteristic curve (AUC) was 0.998 for *N. haitanensis* and 0.992 for *N. yezoensis*, indicating high modelling accuracy. Sea surface temperature contributed mainly to the models. In addition to the predominant distribution in their native habitats in Northwest Pacific, high suitability along the east coast of North America and *trans*-hemispheric distribution was predicted for both species. In 2050 s, high-latitudinal and offshore expansion was observed, increasing over the present distribution area by 10.75%~26.13% for *N. haitanensis* and 18.97%~26.48% for *N. yezoensis*. Current geographic distribution centroid of *N. yezoensis* was located in Seocheon and the centroid shifted northeastward to the Sea of Japan in 2050 s. The most specific haplotypes or high genetic variations (based on chloroplast *rbc*L sequences) were identified in both regions. Current and future centroids of *N. haitanensis* were located in East China Sea, where the highest genetic diversity was identified. The overall haplotype and nucleotide diversity of both species was at low levels while the haplotype distribution showed spacial heterogeneity, more diversified at the convergence zones of warm and cold ocean currents. The overlapping between *N. yezoensis* and *N. haitanensis* geographic distribution centers and species' genetic diversity hotspots implied their ability to adapt to future climate change. These findings provided vital information for conservation and sustainable utilization of these important intertidal seaweeds to address the global climate challenges.

1. Background

Global organisms are undergoing increasing pressure from environmental change caused by human activities. Emission of large amounts of greenhouse gas leads to climate warming (Olischläger et al., 2012). Under current global warming, the marine biogeochemical cycles and ecosystems are stressed by rising temperatures, ocean acidification and ocean deoxygenation (Gruber, 2011). Direct effects of the changes in ocean temperature and chemistry may alter the physiological functioning, environmental adaptability and interaction between marine lives (Doney et al., 2011; Bopp et al., 2013). Studies have shown that marine species respond to ocean warming by changing the latitudinal range of their distribution (Parmesan, 2006; Mueter and Litzow, 2008), leading to local shrinkage or expansion of populations (Cheung et al., 2009; Doney et al., 2011).

Species distribution models (SDMs) have become increasingly

* Corresponding author at: Key Laboratory of Sustainable Development of Marine Fisheries, Ministry of Agriculture and Rural Affairs, Yellow Sea Fisheries Research Institute, Chinese Academy of Fishery Sciences, Qingdao, China.
E-mail address: wjwang@ysfri.ac.cn (W. Wang).

https://doi.org/10.1016/j.ecolind.2023.110219
Received 20 December 2022; Received in revised form 31 March 2023; Accepted 3 April 2023
Available online 7 April 2023

applicable in conservation and management of natural resources (Graham et al., 2004; Alahuhta et al., 2011). SDMs combine current occurrence records and habitat data to create models to predict the species' potential habitat and the changes in distribution under current and future conditions (Peterson et al., 2002; Thuiller et al., 2005). SDMs have been widely used in the research of biological introduction and cultivation (Jueterbock et al., 2013), species protection and biological invasion prevention (Thuiller et al., 2005), and species migration caused by climate change (Verbruggen et al., 2013). The maximum entropy model (MaxEnt) is a SDM originating from the statistical mechanics, and is a general purpose environmental model for predicting the potential distribution of species (Phillips and Dudík, 2008). It uses the maximum entropy algorithm and incidence of species to estimate the likelihood of incidence of species in unidentified event regions. MaxEnt is not susceptible to sample size, can produce species response curves in comparison to environmental variables (Khanum et al., 2013), obtains high prediction accuracy in the context of only species presence information (independent of absence information) (Elith et al., 2006), and is currently an ideal and popular SDM used to predict species distribution (Gebrewahid et al., 2020; Hirabayashi et al., 2022; Xian et al., 2022; Song and Li, 2023).

As primary producers in the ocean, seaweeds are foundational 'ecosystem engineers' (Jones et al., 1996), providing food, habitat, and protection for a diverse range of organisms (Carss and Elston, 2003; Harley et al., 2006; Jueterbock et al., 2016). As carbon sinks, seaweeds play important roles in regulating the marine environment and climate change (Mineur et al., 2015). Seaweeds also have an important economic value for people (Mineur et al., 2015). They have been industrially used in countries such as India, China, Japan and Korea, where they are used to make kinds of seaweed extracts, to feed aquatic animals and to make nutritious and delicious food. Laver, a collective name for bladed Bangiales, are distributed from tropical to cold temperate oceans and have been found on the coastlines of all major land masses (Yang et al., 2017). They are the most important economic seaweeds in Northeast Asian countries China, Korea and Japan (Blouin et al., 2011; Yang et al., 2017; Kim et al., 2022). Two laver species are commercially cultivated in China, *Neoporphyra haitanensis* and *Neopyropia yezoensis*. *N. haitanensis* is a subtropic species endemic to China. *N. yezoensis* is a temperate species, naturally distributed in Northwest Pacific, along the coasts of North China, as well as Japan and Korean Peninsula (Yang et al., 2017, 2018; Kim et al., 2022). Owing to the high species richness and complex geological history, the Northwest Pacific has been a hotspot for seaweed biodiversity study (Hu et al., 2017), especially for laver in recent years (Yang et al., 2018, 2020; Koh and Kim, 2020; Kim et al., 2022). The Northwest Pacific has been suggested to be the centre of origin for modern distribution of *Pyropia/Neopyropia* since the early Cenozoic due to the high biodiversity and the most endemic species (Yang et al., 2017; Kim et al., 2022). However, the species richness and biodiversity of seaweed in Northwest Pacific has been destroyed by environmental changes in the past few decades (Tanaka et al. 2012; Hu et al. 2017). As intertidal seaweeds, the growth and development of laver are affected by various environmental factors (Davison and Pearson, 1996), among which temperature is one of the most important ones (Blouin et al., 2011; Kim et al., 2022). Under the scenario with the lowest concentration of greenhouse gas emission, the global average sea surface temperature (SST) is estimated to rise by 0.4 ~ 1.6 °C in the next two decades (Zhou et al., 2015), which will lay a great impact on laver with regard to species biodiversity, population richness, phylogeographic and geographic distribution, thereby affect the industry.

There is an increasing focus on modelling to predict the impacts of climate change on seaweeds (Araújo et al., 2005; Graham et al., 2007; Wernberg et al., 2011; Tyberghein et al., 2012; Verbruggen et al., 2013; Li et al., 2021). In this study, the geographic and phylogeographic distribution of *N. haitanensis* and *N. yezoensis* were investigated to evaluate present distribution and future shift. Phylogeography is a field of study concerned with the principles and processes governing the geographic distributions of genealogical lineages-typifying the spatial distributions of genotypes within and among closely related species (Avise, 2000). Phylogeography aims to investigate the relationship among geographic history, biogeography, and the mechanisms driving speciation (Avise, 2009; Marc and Xavier, 2020). We hope this study would contribute to the conservation and sustainable use of these important intertidal seaweeds to address the global climate challenges.

2. Methods

2.1. Occurrence records

A total of 579 occurrence records for *N. haitanensis* and 1192 records for *N. yezoensis* were obtained from the Global Biodiversity Information Facility (GBIF) (https://www.gbif.org/) from 1950 to 2022. The duplicate and undefined (without definite coordinates) records were removed from the data set at first. Although MaxEnt has good predictive power with smaller sample sizes relative to other models, different studies have found that a sample size ≤ 30 can lead to inaccurate predictions (Wisz et al., 2008). Additional 28 records of *N. haitanensis* and 40 records of *N. yezoensis* based on our field sampling were subject for screening. We built a buffer around each distribution point according to the environmental data (5 arcmin) to ensure that each grid (9.2 km × 9.2 km) has one distribution point to reduce sampling bias (Steen et al., 2021). Finally, 31 presence records of *N. haitanensis* and 108 presence records of *N. yezoensis* were screened (Tables S1 and S2).

2.2. Environmental variables

N. haitanensis and *N. yezoensis* grow on intertidal zones. We used all 'surface' variables from Bio-ORACLE (https://bio-oracle.org/) (Tyberghein et al., 2012; Assis et al., 2017). We selected the data between 2000 and 2014 as the current climate and the 2040–2050 layers as the future climate. The layers for the future were developed under the representative concentration pathway (RCP) (van Vuuren et al., 2011). Three representative concentration pathways (RCP 2.6, 4.5, 8.5) in 2050 s were compared with the present climatic condition. The data were set at 5 arcmin (about 9.2 km) spatial resolution and downloaded as *.asc format, which were converted using ArcGIS version 10.2. The contribution percentage and permutation importance analysis of environment variables was performed using MaxEnt version 3.4.1. First, the environmental factors with contribution percentage of '0' were removed and a total of 12 environment variables were obtained (Table 1). Second, to determine and exclude extremely correlated variables, the ENMTools version 1.3 was used to perform correlation analysis between the 12 variables. The correlation coefficient $|R|<0.8$ is used as a cutoff to minimize the effect of multicollinearity and model overfitting (Elith et al., 2010). Finally, the variable with the highest contribution percentage was selected from those variables with $|R|>0.8$ (Fig. S1) and

Table 1
Environment variables for MaxEnt modeling.

Environment Variable	Variable Type
Bio 1	Light at bottom. Max ($E/(m^2 \cdot d)$)
Bio 2	Light at bottom. Mean ($E/(m^2 \cdot d)$)
Bio 3	Light at bottom. Min ($E/(m^2 \cdot d)$)
Bio 4	Salinity. Max (PSS)
Bio 5	Salinity. Mean (PSS)
Bio 6	Salinity. Min (PSS)
Bio 7	Temperature. Max (°C)
Bio 8	Temperature. Mean (°C)
Bio 9	Temperature. Min (°C)
Bio 10	Currents velocity. Max ($m \cdot s^{-1}$)
Bio 11	Currents velocity. Mean ($m \cdot s^{-1}$)
Bio 12	Currents velocity. Min ($m \cdot s^{-1}$)

Note: 'max' means maximum record; 'mean' means the long-term average; 'min' means minimum record.

used for MaxEnt modelling to avoid overfitting (Li et al., 2021).

2.3. Optimization of model parameters

The MaxEnt model simulates a range of distributions between potential and realistic distributions. The default parameters were set by simulating data of 266 species from 6 different geographical regions (Phillips and Dudík, 2008), nevertheless, default MaxEnt modelling methods may result in overly complex models with poor transferability (Wiltshire and Tanner, 2020). Thus, it still needs to be adjusted according to different purposes. In this study, the complexity of MaxEnt under different combinations of the regularization multiplier (RM) and the feature class (FC) parameters was analyzed and the combination with the least complexity was selected (Zhu and Qiao, 2016). A total of 1240 parameter combinations, representing all combinations of 40 RM settings (from 0.1 to 4 with 0.1 intervals) and 31 FC combinations were evaluated using R version 3.6.3. The model with the smallest Akaike information criterion correction (AIC) value (AICc) is optimal (Akaike, 1998). Based on the AICc (Fig. S2), the best settings of FC and RM were obtained (Table 2). Data independent from those used to train the model are essential to evaluate the predictive performance of the model (Gebrewahid et al., 2020). In this study, the default 75% of total occurrence data were used as the training set and 25% were used as the test set.

Receiver operating characteristic curve (ROC) plot was used to evaluated the models by calculating the AUC (Area Under the Curve) value. AUC is the area enclosed by the ROC curve and the abscissa. It is a general model performance measure, with the value between 0 and 1. The closer the AUC is to 1, the more accurate the model will be (Fielding and Bell, 1997).

The jackknife test was used to assess the dominant environmental variables that determined the species potential distribution (Yang et al., 2013). Species response curves were created to investigate the relationship between target species habitat suitability and environmental factors, which depict the relationship between environmental variables and the probability of species incidence, and can reflect the biological tolerances for target species and habitat preferences.

2.4. Current and future prediction of N. haitanensis and N. yezoensis distribution

The filtered laver occurrence data (*.csv) and screened environmental data (*.asc) were imported into MaxEnt version 3.4.1, then 10 runs were made for each laver species using the optimized settings as shown in Table 2. The fitness indices, representing the potential suitable distribution range of *N. haitanensis* and *N. yezoensis*, were obtained. Fitness indices (range from 0 to 1) >0.5 indicates the environment is very suitable for the species to inhabit. Four grades were used here: high suitability (>0.5), medium suitability (0.3 ~ 0.5), low suitability (0.05 ~ 0.3) and no suitability (<0.05) (Martín-García et al., 2014).

The SDMtoolbox version 2.5 was used to calculate the distribution change and centroid shift under different scenarios (Brown et al., 2017). The prediction results of *N. haitanensis* and *N. yezoensis* were converted into binary grid files by ArcGIS version 10.2 and SDM toolkit. Then, the expansion, stability, and contraction area of *N. haitanensis* and *N. yezoensis* under the future scenarios was calculated by comparison with the present. The 'Centroid Changes (Line)' tool was used to calculate the geometric center of the predicted distribution under different scenarios so that the overall change of the distribution of *N. haitanensis* and *N. yezoensis* was detected.

Table 2
MaxEnt optimization parameter setting for *N. haitanensis* and *N. yezoensis*.

Protocol	Species	FC	RM	Test set percentage	Number of iterations repeated
Default	/ /	L, Q, T, P, H	1	25	1
Optimized	*Neoporphyra haitanensis*	L, Q	0.1	25	10
	Neopyropia yezoensis	Q, T, P	0.7	25	10

Abbreviations: FC, feature classes; RM, regularization multiplier; H, hinge; L, linear; P, product; Q, quadratic; T, threshold.

2.5. Phylogenetic and haplotype distribution analysis based on rbcL sequences

Among the varying DNA sequences that have been applied for Bangiales, *rbc*L is appropriate for species delineation and phylogeographic analysis due to its moderate evolution rate and the lots of reference data in GenBank (Kim et al., 2018; Koh and Kim, 2020; Kim et al., 2022). Thus, we used the *rbc*L sequences for phylogeographic profiling. The chloroplast *rbc*L sequences of *N. haitanensis* and *N. yezoensis* were downloaded from GenBank, aligned and manually edited with MEGA 11. The segregating sites (S), haplotypes (H), haplotype diversity (Hd), and nucleotide diversity (Nd) were measured with DnaSP 6.0. The parsimony networks of haplotypes were generated with NETWORK 10.2 based on median-joining method. Phylogenetic trees were constructed by MEGA 11 based on maximum likelihood (ML) method and then edited by FigTree 1.4.3.

3. Results

3.1. Model evaluation and importance of environmental variables for current and future prediction

The AUC is an efficient autonomous threshold index capable of evaluating the ability of a model to discriminate presence from absence. The results showed that the 10-repeated average values of AUC were nearly equal to 1 (0.998 for *N. haitanensis* and 0.992 for *N. yezoensis*) (Fig. 1), indicating that the constructed models were reliable and qualified for the following predictions.

Bio 1 (Light at bottom_Max, simplified as max light), Bio 4 (max salinity), Bio 6 (min salinity), Bio 7 (sea surface temperature_max, simplified as max SST), Bio 8 (mean SST), Bio 9 (min SST) and Bio 10 (currents velocity_max, simplified as max velocity) were screened for *N. haitanensis* modelling. Bio 1, Bio 2 (mean light), Bio 3 (min light), Bio 4, Bio 7, Bio 9 and Bio 11 (mean velocity) were screened for *N. yezoensis* modelling.

The jackknife test showed the contributions of the environmental variables were consistent under different climatic scenarios (Fig. S3). Max light contributed the most (34.8% ~ 36.2%) to present and future predictions (Table S3). Max, min and mean SST totally contributed 42.6–43% and min salinity contributed 19.6–20.6% to *N. haitanensis* models. Distribution of *N. yezoensis* was mainly influenced by max salinity, mean and min light, mean and min SST in current and future scenarios while less affected by max light and mean velocity (Table S3). Beside contribution percentage, permutation importance is a significant factor in assessing the environmental variable importance. Permutation importance rather than the path is used in an individual run-up to the final results of the model and therefore is easier for assessing the significance of a particular variable (Gebrewahid et al., 2020). Considering the permutation importance of the variables, the models of both species were extremely determined by SST (95.5% ~ 98.4% and 64.4% ~ 70.1%) (Table S3).

Based on the species response curves acquired under current climatic condition, *N. haitanensis* preferred the max light range from 64 E/(m^2·d) to 71 E/(m^2·d), the min salinity of 16 ~ 27, and the min, mean and max SST of 10–15.5 °C, 19–23 °C and 27.5–29 °C. *N. yezoensis* preferred the min light range from 4 E/(m^2·d) to 15 E/(m^2·d), the mean light of 25–33

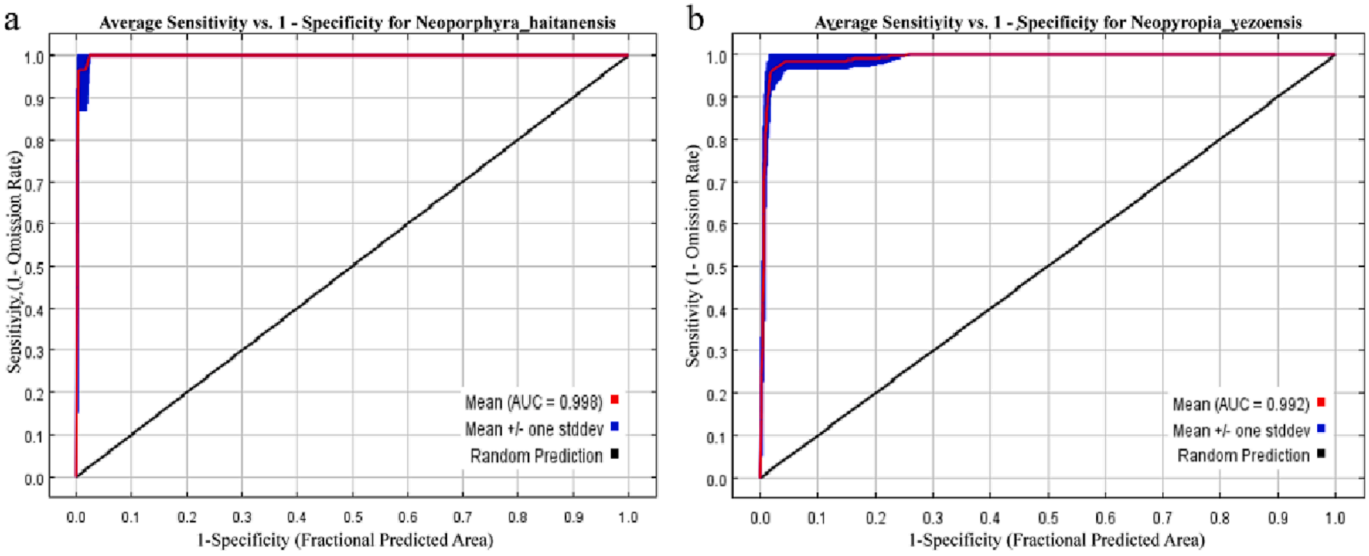

Fig. 1. ROC curve and AUC value of (a) N. haitanensis and (b) N.yezoensis under the current climate (10 replicated runs).

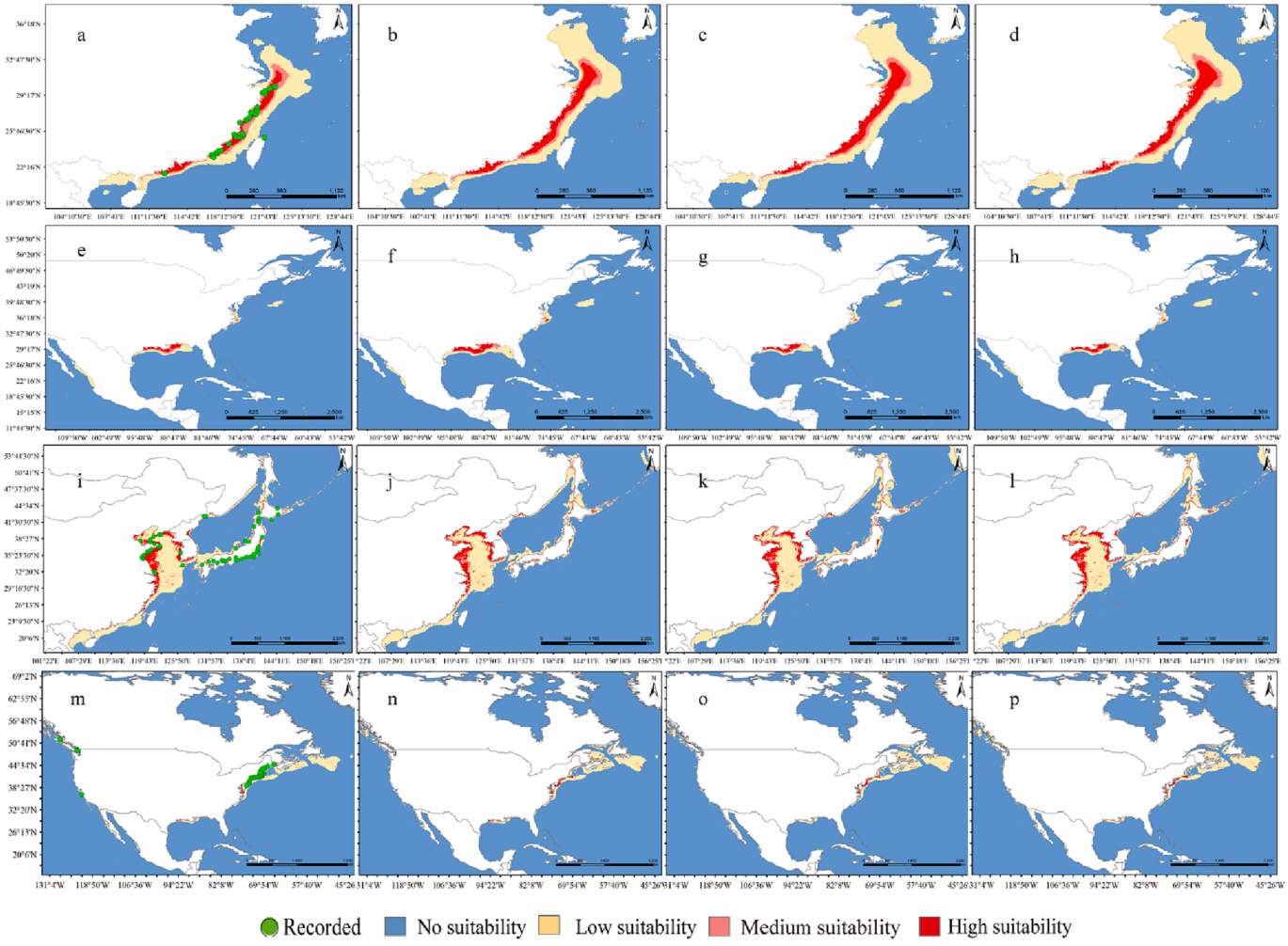

Fig. 2. Potential distribution of the two laver species under present and future climate conditions (2050 s). N. haitanensis under (a) present, (b) RCP 2.6, (c) RCP 4.5, (d) RCP 8.5 in Asia, (e) present, (f) RCP 2.6, (g) RCP 4.5, (h) RCP 8.5 in the United States. N.yezoensis under (i) present, (j) RCP 2.6, (k) RCP 4.5, (l) RCP 8.5 in Asia, (m) present, (n) RCP 2.6, (o) RCP 4.5, (p) RCP 8.5 in the United States.

E/(m^2·d), the max salinity of 40 ~ 44, the min SST range from 2 °C to 4 °C, and the max SST of 20–27.5 °C (Fig. S4).

3.2. Predicted distribution of N. haitanensis and N. yezoensis under current condition

The global potential distribution of both species together with the occurrence data used for modelling was shown in Fig. S5. The occurrence sites in China were screened for *N. haitanensis* modelling (Figs. S5, 2a). The occurrence data used for *N. yezoensis* modelling were mainly from Northwest Pacific, and some from North America were also used (Figs. S5, 2i, 2m).

The constructed models predicted that the current distribution of *N. haitanensis* ranged from 20°N to 34°N and 108°E to 125°E. The high suitable regions generally overlapped the occurrence records. Medium and high potential habitats of *N. haitanensis* would reach to 34°N (North of the Estuary of Yangtze River) (Fig. 2a). A total of 10.75 × 10^4 km^2, 8.99 × 10^4 km^2, and 40.31 × 10^4 km^2 were identified as high, medium and low suitable habitats of *N. haitanensis* in China (Table 3). The predicted high potential habitats of *N. yezoensis* were predominantly distributed along the coast of the Yellow Sea and Bohai Sea in China and the west coast of Korea with about 43.55 × 10^4 km^2 distribution area (Fig. 2i, Table 3). In addition, high distribution of *N. yezoensis* was scattered along the coast of Miyagi and the north of Hokkaido in Japan. The prediction showed that there was a medium potential for *N. yezoensis* to be distributed southward to the coast of Fujian province in China (~24°N). The current distribution would be northward to the coast of Tatar Strait in Russia (~53°N) (Fig. 2i).

In addition to Northwest Pacific, potential distribution of *N. haitanensis* was identified in North America, with about 7.26 × 10^4 km^2 of high suitability in the north of Gulf of Mexico (Fig. 2e, Table 3). High suitability of *N. yezoensis* was situated from the northeastern coast of North Carolina to New York with about 11.54 × 10^4 km^2 distribution area (Fig. 2m, Table 3). There were additional 33.62 × 10^4 km^2 and 155.07 × 10^4 km^2 of medium and low suitable regions for *N. haitanensis* and *N. yezoensis*, respectively, in North America (Table 3). Potential distribution of *N. yezoensis* and *N. haitanensis* was predicted in other regions of the world. Persian Gulf may have high suitability for *N. haitanensis* and low suitability for *N. yezoensis* (Fig. S5). Low suitability of *N. haitanensis* was scattered in the Marmara Sea in Europe and the west coast of Mexico. Medium/low suitability of *N. yezoensis* was scattered in Europe (Black Sea, Baltic Sea, North Sea) and the east coast of Canada. It's noteworthy that low to medium suitability was identified for both species on the east coast of South America (Brazil, La Plata Bay and Branca Bay) and the north coast of Australia (Carpentaria) (Fig. S5).

3.3. Potential distribution of N. haitanensis and N. yezoensis under future climate conditions

Under the future three scenarios, the potential distribution of *N. haitanensis* and *N. yezoensis* was still predominantly in Northwest Pacific and North America (Fig. 2). There would be expansion and contraction of the geographic distribution of both species in the future, with expansion much greater than contraction (Fig. 3). In total, future scenarios would increase over the current distribution by 10.75% ~ 26.13% for *N. haitanensis* and 18.97% ~ 26.48% for *N. yezoensis* (Table 4).

Compared to current scenario, the future scenarios would increase the high suitable distribution of *N. haitanensis* by 1.44 ~ 1.60 folds (Table 4, Figs. 2 and 3). Offshore and northward expansion of high suitable area would occur in Northwest Pacific (Fig. 2b-d). In addition, the low suitable distribution region expanded northward significantly (Fig. 3). Under RCP 2.6–2050 s and RCP 8.5–2050 s, there was even offshore expansion along the coast of Guangxi province (~19°N). In North America, there was significant offshore expansion of *N. haitanensis* distribution at high latitude (Fig. 2f-h). The future scenarios would increase the high, medium and low suitable regions of *N. yezoensis* by 1.14 ~ 1.16, 1.26 ~ 1.33, and 1.19 ~ 1.27 folds, respectively (Table 4, Figs. 2 and 3).

3.4. Shift of the distribution centroid under future climate conditions

Both the current and future Northwest Pacific centroids of *N. haitanensis* were located in East China Sea, which was currently located in Wenzhou (27.29°N, 121.19°E) and shifted to Taizhou (28.78°N ~ 29.30°N, 121.52°E ~ 122.15°E) in 2050 s (Fig. 4a). The current distribution centroid of *N. yezoensis* was located in Seocheon, South Korea (35.99°N, 126.54°E). In 2050 s, the centroid shifted to the Sea of Japan (37.96°N ~ 38.56°N, 128.83°E ~ 129.61°E) (Fig. 4b).

3.5. Haplotype distribution of N. haitanensis and N. yezoensis based on rbcL sequences

The abbreviation, location/source, haplotype of sequences were shown in supplementary data Table S4.

For *N. haitanensis*, 52 *rbc*L sequences with the length of 1315 bp were obtained. Twenty-six segregating sites and 12 haplotypes (H1 ~ H12) were identified, with haplotype diversity (Hd) of 0.494 and nucleotide diversity (Nd) of 0.00166. The most abundant haplotype was H3, shared by 37 samples (Fig. 5a). H2, H4 and *H*11 were shared by 2 ~ 3 individuals, and the other 8 haplotypes were represented by single sample. Except H1 and H2 that experienced over ten putative steps of mutation from *H*11, the other haplotypes including *H*11 all experienced 1 ~ 3 steps of mutation from H3 (Fig. 5a). The phylogenetic tree also showed that the individuals (JN1, JN2-1/2) characterized by H1 and H2 were mostly divergent from the others and the second highest divergent group (CN10) was characterized by *H*11 (Fig. 5b). All 52 sequences came from 19 geographically separate locations (Fig. 5c). H3 was the most widely distributed haplotype, shared by 14 locations. Among the 10 location-specific haplotypes, eight were distributed in China. The largest number (8 out of 12) of *N. haitanensis rbc*L haplotypes was identified in Zhejiang province, China (118°01′~123°10′E, 27°02′~31°11′N) (Fig. 5c).

For *N. yezoensis*, 123 *rbc*L sequences with the length of 1019 bp were obtained. Twenty-four segregating sites and 20 haplotypes (H1 ~ H20) were identified, among which 12 haplotypes were represented by single sample. The identified haplotypes were divided into two major clusters with H2 and H3 as the centers respectively (Fig. 6a). H2 was the most abundant haplotype, shared by 62.60% of the total individuals. H3 was shared by 14 individuals. H17 experienced the maximum steps of mutation from H3. The phylogenetic tree also showed that the samples (CN1-1 ~ 7, CN2-1, CN3-12) characterized by H15 ~ H17 was highly

Table 3
Distribution area of *N. haitanensis* and *N. yezoensis* under current climate condition (×10^4 km^2).

Region	*N. haitanensis* high suitability	medium suitability	low suitability	*N. yezoensis* high suitability	medium suitability	low suitability
Asia	10.75	8.99	40.31	43.55	19.79	164.28
North America	7.26	4.94	28.68	11.54	16.63	138.44
Other regions	0.78	1.49	39.45	6.51	32.62	284.29
Total	18.79	15.42	108.44	61.60	69.04	587.01

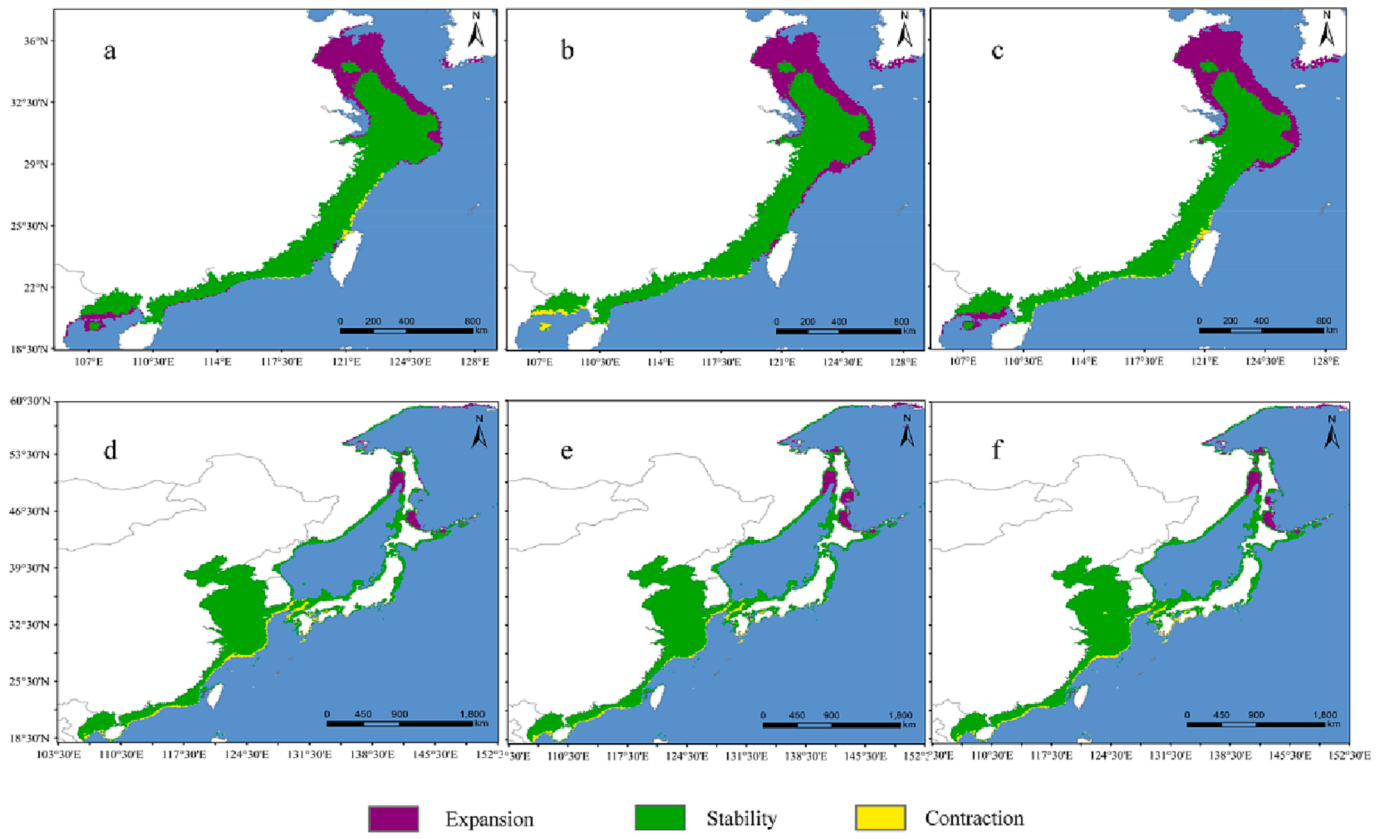

Fig. 3. Shift of the distribution of N. haitanensis and N.yezoensis in Northwest Pacific in 2050 s. N. haitanensis under (a) RCP 2.6, (b) RCP 4.5, (c) RCP 8.5, N. yezoensis under (d) RCP 2.6, (e) RCP 4.5, (f) RCP 8.5.

Table 4
Current and future distribution area of *N. haitanensis* and *N. yezoensis* and the changes in Northwest Pacific under future climatic conditions ($\times 10^4$ km^2).

Current and future distribution	*N. haitanensis* high suitability	medium suitability	low suitability	*N. yezoensis* high suitability	medium suitability	low suitability
Current	18.79	15.42	108.44	61.60	69.04	587.01
2050-RCP2.6	26.99	14.82	127.48	70.41	86.97	696.40
2050-RCP4.5	27.06	14.61	116.32	71.74	92.08	707.47
2050-RCP8.5	30.11	17.44	132.38	71.19	91.47	744.99
Changes in Northwest Pacific	***N. haitanensis***			***N. yezoensis***		
	Expansion	**Stability**	**Contraction**	**Expansion**	**Stability**	**Contraction**
2050-RCP2.6	14.37	41.06	0.73	22.39	215.30	12.32
2050-RCP4.5	15.64	40.50	1.29	34.15	217.18	10.44
2050-RCP8.5	19.01	40.77	1.03	30.47	215.89	11.73

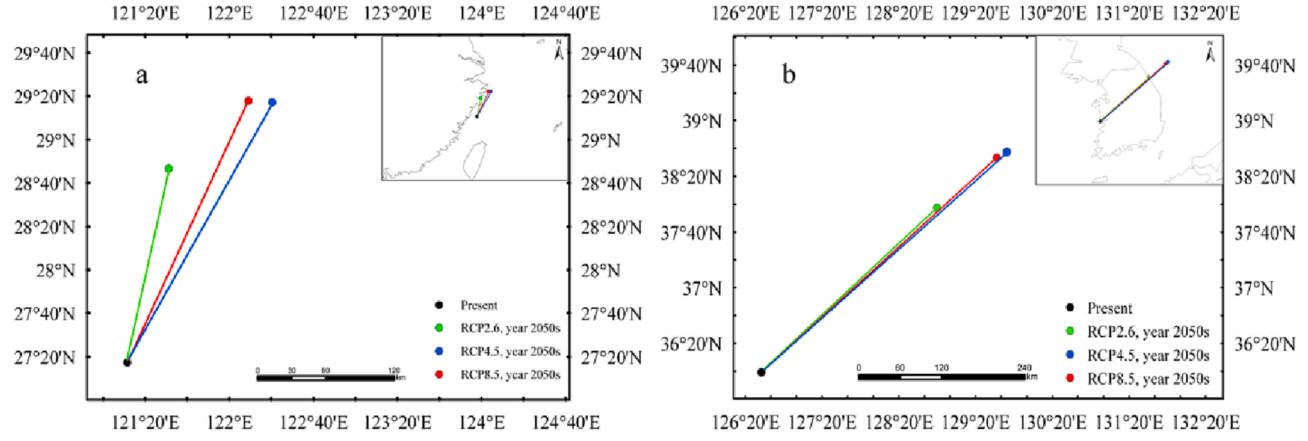

Fig. 4. Shift of the distribution centroid of (a) N. haitanensis and (b) N.yezoensis under future climate conditions.

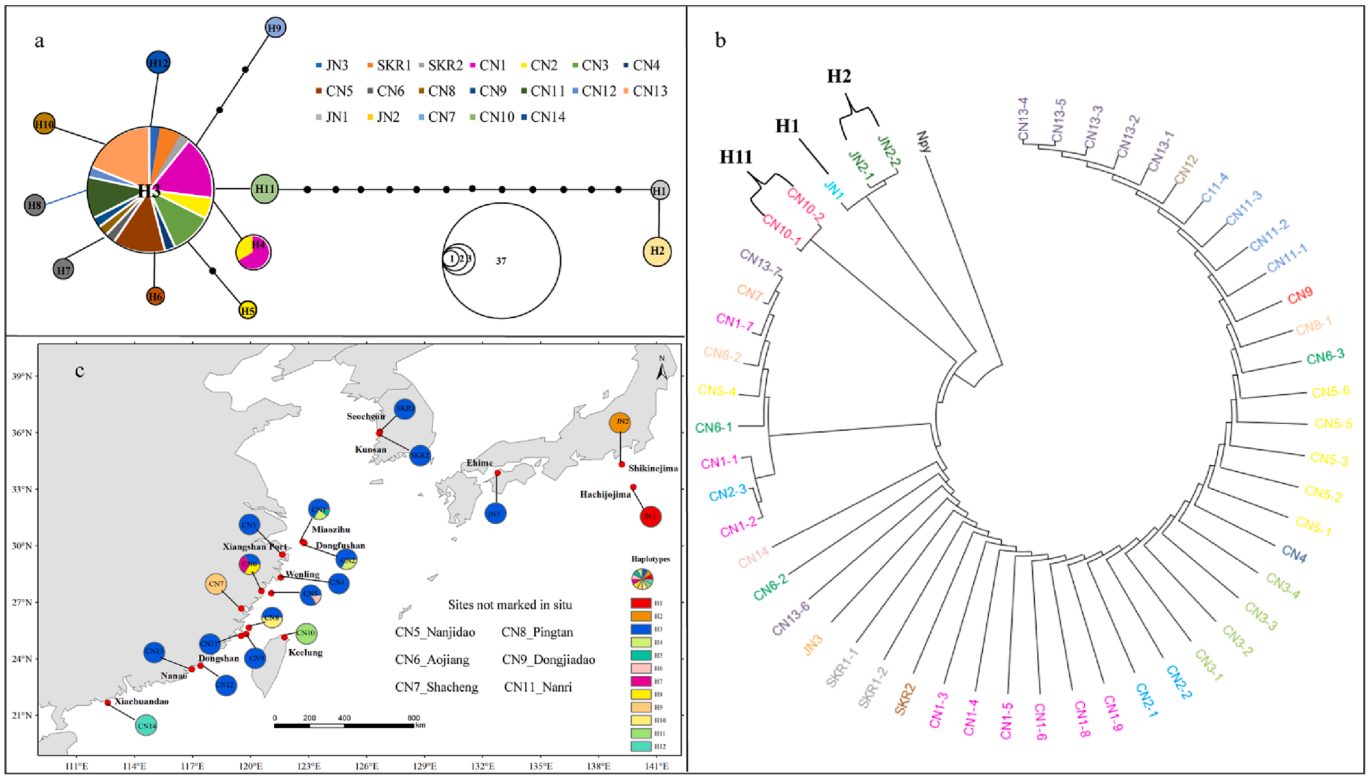

Fig. 5. Parsimony network of haplotypes (a), phylogenetic tree (b) and geographic distribution of haplotypes (c) based on N. haitanensis rbcL sequences. In (a): each link between haplotypes represented one mutational difference; unlabeled nodes indicated inferred steps not found in the sampled populations. Regional distribution of haplotypes: China = H3 ~ H12; South Korea = H3; Japan = H1 ~ H3. In (b): Npy-Neopyropia yezoensis.

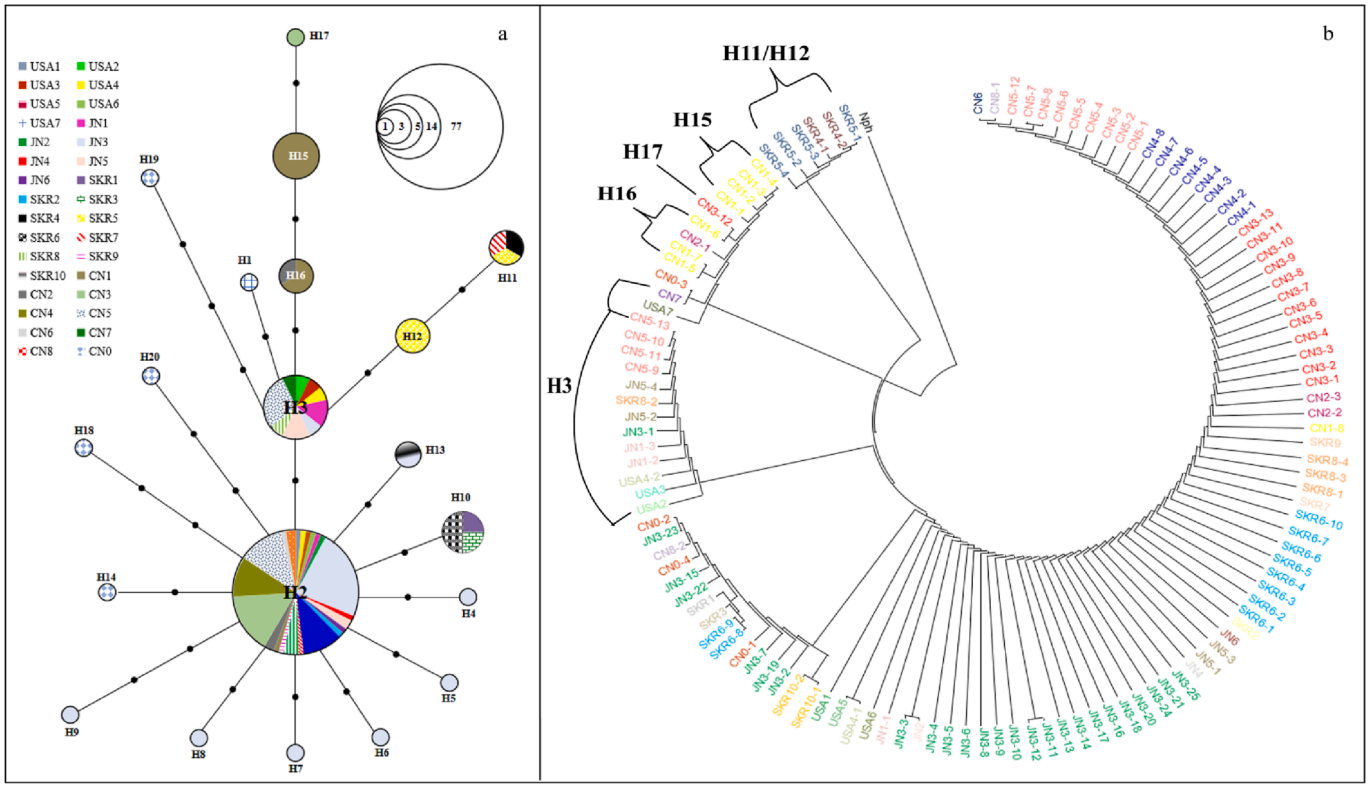

Fig. 6. Parsimony network of haplotypes (a) and phylogenetic tree (b) based on N. yezoensis rbcL sequences. Regional distribution of haplotypes: China = H2 ~ H3, H14 ~ H20; South Korea = H2 ~ H3, *H*10 ~ H13; Japan = H2 ~ H9, USA = H1 ~ H3. In (b): Nph-Neoporphyra haitanensis.

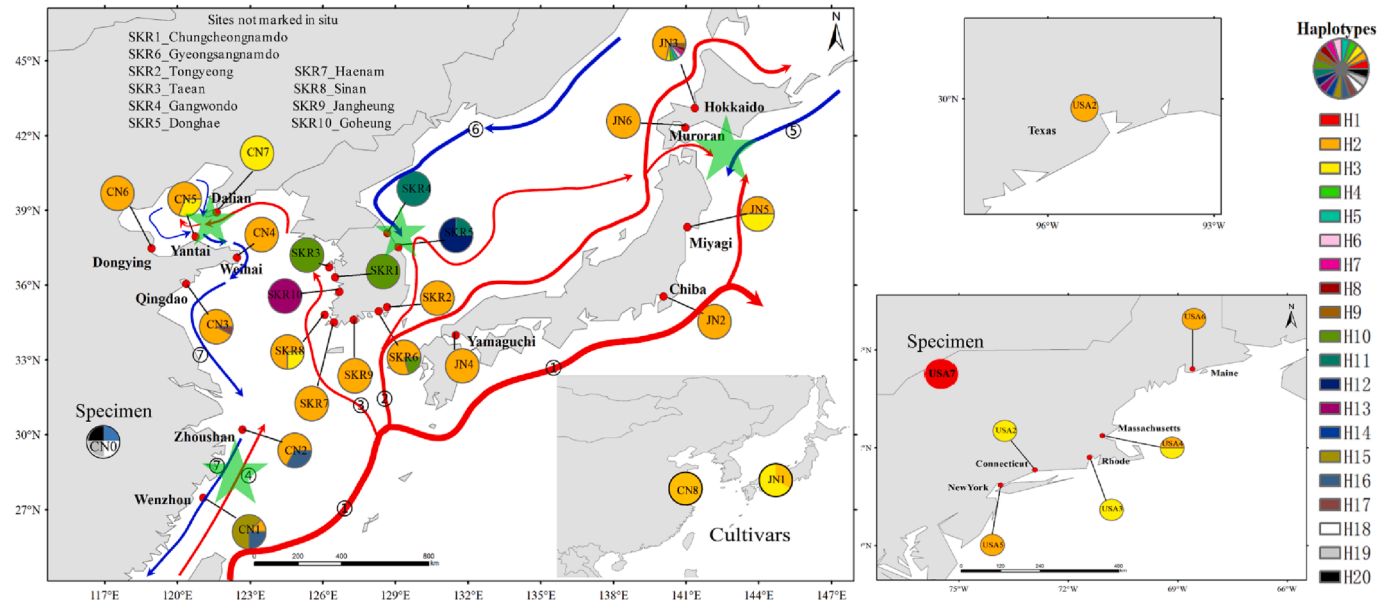

Fig. 7. Geographic distribution of N. yezoensis rbcL haplotypes. Red and blue arrow lines showed warm and cold sea currents respectively: ①Kuroshio Current, ②Tsushima Current, ③Huanghai Current, ④Taiwan Current, ⑤Oyashio Current, ⑥Liman Current, ⑦China Coastal Current. Green star showed convergence zones between cold and warm currents.

divergent from the others (Fig. 6b), which came from East China Sea (Zhejiang province) (Fig. 7). *H*11 and H12 were the most divergent from the others based on the phylogenetic tree (Fig. 6a, b) and were specifically distributed on the north coast of South Korea (SKR4, SKR5) (Fig. 7). H1, H14, H18 and H19 were represented by single specimen (most likely herbarium) without geographic sampling or cultivar information. Except 5 cultivar and 5 specimen samples, the other 113 *N. yezoensis* sequences came from 28 geographically separate locations. H2 was the most widely distributed haplotype, shared by 20 locations (Fig. 7). Totally, there were 9 haplotypes in China, 8 in Japan, 6 in South Korea and 3 in USA. In Japan, except the widely distributed H2 and H3, the specific haplotypes were all identified in Hokkaido.

Considering Hd and Nd indices, the *N. yezoensis* groups from Zhejiang, China (CN1, 2/H2, 15, 16) had the highest Hd (0.709) and Nd (0.00144); those from the west coast of South Korea (SKR1, 3, 10/*H*10, 13) was the second highest Hd (0.6) and Nd (0.00103); the third highest Hd (0.6) and Nd (0.00052) was represented by the groups from the north coast of the South Korea (SKR4, 5/*H*11, 12). All haplotypes present in Japan were identified in Hokkaido. Taking ocean current into account, it was found here that the haplotypes were identified in a large number or at a high divergence level at the convergence regions of cold and warm currents, i.e., between Taiwan Current and China Coastal Current, Tsushima Current and Liman Current, Kuroshio Current and Oyashio Current (Fig. 7). It was interesting that the individuals with H3 haplotype in China were all distributed at the intersection of the Yellow Sea and the Bohai Sea (i.e., CN7: Dalian and CN5: Changdao, Yantai). In other words, 5 out of 6 sequences from this region were characterized with H3 haplotype. The phylogenetic tree showed that all H3 individuals were grouped into a clade and separated from the others (Fig. 6b).

4. Discussion

Laver is a global popular food based on its high mineral, vitamin and protein content (Blouin et al., 2011; Liang et al., 2022a). Mariculture of laver is an important component of aquaculture in China, Japan and Korea (Yang et al., 2017; Kim et al., 2022). The wild harvest of laver collected historically from Atlantic shores continues today in Great Britain, Ireland, Canada and the United States (Blouin et al., 2011). *N. yezoensis* and *N. haitanensis* are predominant cultured laver species (Kim et al., 2022; Liang et al., 2022b; Yang et al., 2017). It is predicted that climate change will cause emergent global challenges to marine ecosystem in the coming decades (Marien and Michael, 2011). Climate change has been laying great impact on species biodiversity, population richness, phylogeographic and geographic distribution. For instance, *Neopyropia tenera* was one of the main aquaculture species in Korea and Japan but gradually disappeared from both natural habitats and aquaculture farms (Kim et al., 2022).

4.1. Distribution center of *N. yezoensis* and *N. haitanensis* in Northwest Pacific

Based on the species richness biodiversity, and the number of endemic species, Northwest Pacific has been suggested to be the center of origin for modern distribution of some laver taxons, among which *N. yezoensis* and *N. haitanensis* are two endemic species (Yang et al., 2017; Kim et al., 2022). Especially, *N. haitanensis* has long been considered as an indigenous species of China (Yang et al., 2017). Thus, only the occurrence records in China were used for *N. haitanensis* modelling in this study, with the most came from our field survey in recent several years (Fig. 2a) so as to project a more realistic prediction for present climate.

Based on modelling prediction, the geographic distribution centers of both species were drawn. It was interestingly found that there was some homologous characteristics of the phylogeographic pattern based on *rbc*L sequences. The current and future centroids of *N. haitanensis* were located in the coastal area of Zhejiang Province in China (Fig. 4a). The most *N. haitanensis* haplotypes were identified in this region, accounting for 2/3 of the total identified haplotypes of this species (Fig. 5c). The haplotype diversity (Hd) of the Zhejiang group (0.572) was higher than that of the species overall level (0.494). Nonetheless, the nucleotide diversity (Nd) indices at both group and species level were < 0.005. According to Grant and Bowen (1998), when Hd is < 0.5 and Nd is < 0.005, the population should have experienced bottleneck effect or builder effect; when Hd is > 0.5 and Nd is < 0.005, the population possibly has encountered bottleneck effect, followed by rapid population expansion and accumulation of variation. Thus, *N. haitanensis* should have experienced bottleneck effect. This may be a result of paleontological event (Yang et al., 2017). Bangiales is a group

of ancient and primitive red algae (Blouin et al., 2011). The evolutionary rates are supposed to be dramatically faster in red algae than in land plants and green algae, however, they are slower in Bangiales than in Florideophyceae. The relatively low evolutionary rates at the nucleotide level lead to low speciation rate of Bangiales (Xu et al., 2018). *N. haitanensis* may be a more recently diverged lineage in red algae (Ca. 204 Myr) (Cao et al., 2020). At early Cenozoic (Ca. 60 Myr), ancient species were driven from three centers of origin (i.e., Antarctic, North Pacific and Indo-West Pacific), species arose after splitting from ancestral species when they acquired new adaptations to a changing environment, thereby antitropical distributions of many modern species was formed (Briggs, 2003). During Pliocene and Pleistocene (12 ~ 2.5 Myr), rapid climatic fluctuations caused either complete extinction or range contraction to fragmented refuges with severe bottlenecks, thereby instigated genetic divergence and sympatric speciation (Allcock and Strugnell, 2012; Guillemin et al., 2018; Kim et al., 2022). Thus, we speculated that *N. haitanensis* should have had refuges in East China Sea. Our results suggested that the centers of geographic distribution and genetic diversity of this species are both located in East China Sea (Zhejiang province). Many ancient Chinese books have recorded universal distribution of laver along East China Sea, which can be traced back to ~ 1700 years ago. At least 500 years ago, the ancient Chinese began to culture laver from many coastal counties in Fujian province. *N. haitanensis* was named in memory of the ancient cultivation method (Yang et al., 2017).

The occurrence of *N. haitanensis* in Korea and Japan seemed to be introduced from China. Our prediction based on MaxEnt modelling didn't identify suitable habitats for *N. haitanensis* in Japan and Korea under present climate (Fig. S5a). A total of 7 *rbc*L sequences were obtained from South Korea and Japan. Except 3 sequences from Japan were characterized by H1 and H2, all the other sequences belonged to H3—the predominant haplotype in China (Fig. 5). The samples characterized by H1 (from Hachijojima) and H2 (from Shikinejima) were the first record of natural *N. haitanensis* in Japan, which was genetically different from those from China (Sano et al., 2021). The haplotype network and the phylogenetic tree showed that H1 and H2 were derived from *H*11, a specific haplotype on the northeast Taiwan coast (Fig. 5c). These locations were just on the way of the Kuroshio Current (see the current distribution in Fig. 7). *N. haitanensis* has been introduced from China to Japan for experimental cultivation in areas such as Yamaguchi (Sano et al., 2021). Thus, the distinct genetic profile between samples with H1/H2 and those with H3 in Japan and Korea seemed to be due to different introduction pathways, with the former introduced by ocean current at a long timescale and the later introduced by human activities at a recent timescale.

The present findings with regard to the high genetic diversity of *N. yezoensis* in the East China Sea and the large number of haplotypes in Hokkaido was in consistent with the previous report (Koh and Kim, 2020). It was interesting that there is strong convergence of warm and cold ocean current in these two regions, namely Taiwan Current vs China Coastal Current and Kuroshio Current vs Oyashio Current. We further found that the sequences from the north coast of Korea (the Sea of Japan) were grouped into a clade positioned at the base of the phylogenetic tree (Fig. 6b). A distinct haplotype composition was also identified in *Phycocalidia suborbiculata* in the Sea of Japan (Koh and Kim, 2020). The divergence may be derived from environmental isolation such as terrestrial partition and convergence between Tsushima Current and Liman Current (Koh and Kim, 2020). Interestingly, all H3 individuals identified in China were distributed around the intersection of the Yellow Sea and the Bohai Sea (Fig. 7). All the above indicated that ocean current contributes significantly to genetic diversification of *N. yezoensis*. Based on modelling prediction, the geographic centroid of *N. yezoensis* was in the Yellow Sea (Seocheon, the west coast of South Korea) at present and shifted to the Sea of Japan under the three future scenarios (Fig. 4b). The phylogeographic distribution of this species showed that the west coast of South Korea had the highest number of haplotypes in the Yellow Sea (Fig. 7) and the groups of SKR1, 3, 10 had the second highest Hd (0.6) and Nd (0.00103). In sum, the geographic centroids of *N. yezoensis* were just located where the populations were genetically diversified.

In general, the larger the population, the higher the genetic diversity, the stronger ability to defend against adverse conditions, and the more stable the population. The overlapping between the geographic distribution centers and the genetic diversity hotspots of *N. yezoensis* and *N. haitanensis* implied their ability to adapt to future climate change. An experiment simulating global warming indicated ocean acidification improved the tolerance of *N. haitanensis* to high temperature and strong irradiance, thus speculated that laver aquaculture may benefit from ocean acidification under global warming (Li et al., 2021).

4.2. Potential distribution of *N. yezoensis* and *N. haitanensis* in North America and Europe

According to the MaxEnt models, suitable habitats of both species were identified in other parts of the world, especially in North America where considerable regions were predicted as high suitability for both species (Fig. 2e, m, Table 2). High distribution of *N. haitanensis* was predicted in the Gulf of Mexico, where occurrence of this species was reported in 2021 (Bombin et al., 2021). Nowadays, ocean shipping is continuously growing, which may elevate the potential of transporting alien species to new localities (Sheehy and Vik 2010; Bieler et al., 2017). Several of the largest American marine trading ports are located in the Gulf of Mexico (Sprung et al., 2018), which would increase the introduction probability of alien species such as *N. haitanensis*. The transoceanic distribution has been observed both at subgeneric and specific levels for considerable laver species and most transoceanic species are considered to be recent introductions via such as shipping (Yang et al., 2018). Field sampling of *N. yezoensis* has been achieved at several sites within the predicted high suitable distribution regions in North America and even in the predicted low suitable region Texas (Fig. 2m, Fig. 7) (West et al., 2005; Neefus et al., 2008; Wynne 2008). Haplotype analysis showed that except a specimen with unknown background, all the *rbc*L sequences sampled in the United States were characterized by H2 and H3, the most abundant and universal haplotypes in Northwest Pacific (Fig. 7), verifying their introduction from Northwest Pacific (Neefus et al., 2008). Except for North America, our prediction identified universal discontinuous low to medium distribution of *N. yezoensis* in Europe, where it has been field-sampled since the 1990 s, especially in recent years (Kornmann and Sahling 1991; Brodie et al., 2015; Anon, 2017; Petrocelli and Cecere 2019; Sfriso et al., 2019). The consistency between our modelling prediction and the field sampling validated the capacity of our models.

MaxEnt is a powerful tool to predict the introduction probability/invasion risk of nonindigenous species (Thuiller et al. 2005; Laeseke et al., 2020). Our models predicted suitable habitats in the regions without occurrence records, e.g., the Persian Gulf. This is possibly due to sampling bias, e.g., lack of survey (Laeseke et al., 2020). *N. haitanensis* and *N. yezoensis* prefer hard substrata (Yang et al., 2017). Our field survey found that *N. haitanensis* usually inhabits steep cliffs or uninhabited islands in South China, where we are hard to land to sample. Potential Southern Hemispheric distribution was identified for *N. haitanensis* and *N. yezoensis*. The distribution of a taxon on both hemispheres has been identified for many floras and faunas including considerable laver species (Briggs, 2003; Yang et al., 2018). Whether there is currently realistic distribution of these species, the present prediction indicated they may settle down once introduced in these regions and even gain range expansion thereby.

4.3. High latitudinal and offshore expansion of *N. yezoensis* and *N. haitanensis* under climate changes

Climate change is having complex and long-lasting consequences for

marine ecosystems (Doney et al., 2011). Global warming will increase glacier melting and rainfall that leads to changes in seawater salinity. Increased seawater temperature causes reduced dissolved oxygen levels and even changes in surface ocean winds that will affect seawater flow rates. The increase in greenhouse gas emissions is causing ocean acidification (Caldeira and Wickett, 2003). The state of sea surface upwelling is weakening due to rising SST (Franco et al., 2018). Rising temperatures will also have an impact on the stratification of the upper mixed layer of the ocean, leading to changes in nutrients, such as iron and nitrogen (Flukes et al., 2015; Murcia et al., 2020). All of these climatic and environmental changes affect marine organisms and could lead to changes in species distribution and marine ecosystem (Guinotte and Fabry, 2008; Popova et al., 2016).

N. haitanensis and *N. yezoensis* naturally inhabit intertidal zones, where they encounter strong fluctuations of climatic and environmental conditions such as temperature, irradiance, salinity, dehydration and rehydration due to tide and ebb (Davison and Pearson, 1996; Blouin et al., 2011; Wang et al., 2016; Kim et al., 2022). Temperature profoundly influences the survival, recruitment, growth, and reproduction of seaweeds (Breeman, 1988). Maximum SST was identified as the main predictor variable for MaxEnt modelling of seaweeds (Jueterbock et al., 2016; Murcia et al., 2020). In this study, SST was also identified to be the main environmental variable for current and future modelling of *N. haitanensis* and *N. yezoensis*. The species response curves plotted the min and max SST for *N. haitanensis* (10 ~ 15.5℃/27.5 ~ 29℃) and *N. yezoensis* (2℃~4℃/ 20 ~ 27.5℃) distribution (Fig. S4). Response curves from SDMs do not always reflect physiological or ecological responses (Wiltshire and Tanner, 2020). The temperature threshold for a laver species differs among different strains, between different life stages and at different growth and development stages. *N. haitanensis* and *N. yezoensis* have heteromorphic biphasic life cycles with alternation between bladed gametophytic stage and filamentous sporophytic stage (conchocelis). Generally, blades of *N. haitanensis* prefer to 16 °C ~ 24 °C and endure up to 30 °C (Li et al., 2021; Ai et al., 2022). Blades of *N. yezoensis* prefer to 10 °C ~ 20 °C. The conchocelis prefers to 20 °C ~ 25 °C and endures 5 °C ~ 30 °C (Kim et al., 2022). Both species are tolerant to low temperatures. During laver culture, the technique 'net-freezing' (stored at ca. −25 °C for months) was universally applied in Japan and China to avoid adverse weather, eliminate unwanted algae (e.g., green algae), and replace the cultivation nets in the sea (Yang et al., 2017). It can be seen that our species response curves generated credible values of environment variables for *N. haitanensis* and *N. yezoensis*.

Rising temperatures were predicted to have low impact on the low-latitudinal limits of temperate species' distribution, but to shift their high-latitudinal distribution limits poleward (Jueterbock et al., 2016). It was consistently found here: there was no obvious change in the southern distribution limit, by contrast, the models predicted overall expansion of distribution in 2050 s for both laver species (Table 3, Figs. 2 and 3). There might be three reasons: 1) both species have a considerable range of temperature adaptation, 2) they have heteromorphic biphasic life cycles and show typical seasonality in abundance and reproduction (Kim et al., 2022), and 3) ocean acidification improves their tolerance to high temperature (Li et al., 2021). The future distribution centroids of both species exhibited poleward and offshore shifts (Fig. 4). Distribution of many species shifted to higher latitudes or higher elevations after the Last Glacial Maxima when the earth warmed gradually (Davis and Shaw, 2001), which continues under current global warming (Parmesan et al., 1999; Parmesan and Yohe, 2003; Vanderwal et al., 2013). The poleward shift of seaweed species in response to increasing temperatures is a contemporary phenomenon documented over the last decade (Wernberg et al., 2011; Jueterbock et al., 2016; Laeseke et al., 2020; Murcia et al., 2020; Wiltshire and Tanner, 2020). For marine species, they may shift not only their latitudinal ranges (Parmesan, 2006) but also depth ranges (Dulvy et al., 2008).

4.4. Insight into future development of laver aquaculture

For economic seaweeds, climate-driven changes in habitat have an immediate effect on mariculture and industry. Compared with offshore regions, nearshore environment is more vulnerable to human activities and be disturbed (Liang et al., 2022b). *N. haitanensis* and *N. yezoensis* naturally grow on rocks or other hard substrata in intertidal zones. There has been no report of floating life of these species as yet. Thus, for these species to naturally occupy offshore regions, there should be hard substrata. Meanwhile, the bottom light may be another limiting factor. The species response curve showed the min light range for *N. yezoensis* distribution was 4–15 E/(m^2·d) (Fig. S4).

Purely mechanistic approaches may generate overestimation by disregarding complex interactions of influencing factors (Mac Nally, 2000). The SDMs generally predict continuous species distribution as in present and previous studies (Jueterbock et al., 2016; Laeseke et al., 2020; Murcia et al., 2020; Wiltshire and Tanner, 2020). The distribution of laver in China is actually discontinuous. There is no record of natural distribution of laver along the coastline of Tianjin, Hebei and Guangxi provinces, as well as on the mid and southern coastline of Jiangsu province (Yang et al., 2017). The type of sediment in the intertidal zone may be one of the causes. The present models as well as the most reported SDMs used for seaweeds (i.e., Jueterbock et al., 2016; Laeseke et al., 2020; Murcia et al., 2020; Wiltshire and Tanner, 2020) didn't take substrate availability into consideration since it is not included in Bio-ORACLE, which may be one of the reasons for the overestimation. Laeseke et al. (2020) created a layer for substratum type "rock/soft" for SDM prediction of *Capreolia implexa*, which occupies a variety of hard substrata. *C. implexa* was predicted to gain habitat on coasts with soft substrate, i.e., substrate availability seemed to have no influence on their prediction (Laeseke et al., 2020). This indicates that SDMs together with the relative public databases need further improvement.

The models using limited variables (for seaweeds, e.g., excluding water depth and substrate types) for prediction are likely to be suboptimal for predicting natural occurrences of a species, e.g., over-predicting in areas where the depth or substrate is unsuitable for a seaweed's natural inhabitation (Wiltshire and Tanner, 2020). Nevertheless, for the seaweeds cultivated through floating raft culture systems where water depth and substrate type can be negligible, the prediction is still of great significance. For example, the MaxEnt predicted a large area of high suitability of *N. yezoensis* in Jiangsu province, China. Jiangsu province is characterized by soft seabed along the coastline, lacks natural distribution of laver, but has been the main farming area of *N. yezoensis* for several decades (Yang et al., 2017). The environmental data used are annual averages or seasonal extremes, thus, SDMs reflect long-term suitability. It is possible that some of the predicted low suitable areas may be suitable to grow at certain times of year and permit seasonal cultivation (Wiltshire and Tanner, 2020), in particular for the species with heteromorphic biphasic life cycles and different life-history stages having different temperature tolerances, such as *N. haitanensis* and *N. yezoensis* (Kim et al., 2022). *N. haitanensis* and *N. yezoensis* spend hot seasons in the form of conchocelis stage (sporophyte) which endure higher temperature than the blade stage (gametophyte) (Kim et al., 2022). During cultivation, conchocelis is cultured indoor during hot seasons and the blade stage is cultured at sea in cool seasons (Yang et al., 2017). Taken together, the present prediction based on MaxEnt modelling provided guidance for *N. haitanensis* and *N. yezoensis* aquaculture under climate change. Expansion of laver farming northward and offshore is not simply a prediction, but a current laver culture practice in China (Li et al., 2018; Liang et al., 2022a; Wang et al., 2016).

4.5. Uncertainty of MaxEnt modelling

Despite the great utility of MaxEnt to predict species' potential distribution, it cannot be ignored that uncertainties are part of any predictive modelling approach (Cheung et al., 2009; Austin and Van Niel,

2011). The MaxEnt model typically assumes that all locations on the background are sampled with the same probability, relying on a sample with no sampling bias. Since lavers are mostly distributed in Northwest Pacific, information on the distribution of lavers in other parts of the world can only be obtained through large databases and references, resulting in sampling bias due to different sampling methods, environmental conditions, and other factors. In addition, the occurrence records exhibit spatial autocorrelation (Phillips et al., 2009; Boakes et al., 2010). In this study, the occurrence data were screened by spatial thinning method to minimize the spatial bias of the model (Steen et al., 2021). As discussed above, the models using limited variables (for seaweeds, e.g., excluding water depth and substrate types) for prediction are likely to be suboptimal for predicting natural occurrences of a species (Wiltshire and Tanner, 2020). Besides, the predictive power of SDMs may be biased when physiology data are excluded from model parameters, or it may lose power when extrapolated to new environments (Evans et al., 2016). It was beyond the scope of this study to include data on *N. haitanensis*' or *N. yezoensis*'s physiology (such as photosynthetic parameters) to model their future range distributions (Murcia et al., 2020).

Complex ecosystems show nonlinear, hysteretic, discontinuous excursions rather than linear, continuous, and reversible changes in response to climate and anthropogenic drivers (Ma et al., 2021). Although the oceans have some self-healing capacity, without immediate efforts to mitigate climate change, the rate of change in marine ecosystems will accelerate in the coming decades (Marien and Michael, 2011). In future, the use of climate-driven environmental change management tools in regional dimensions or the use of remote sensing tools to monitor changes in local-to-local environmental conditions will be strengthened to improve the resilience of marine communities to climate stress and to improve monitoring of abiotic changes.. Although the SDMs may generate some underestimation or overestimation, the ability of each model to predict to independent test data is a valid measure of relative model performance (Wiltshire and Tanner, 2020). Thus, we suggest that except for field validation, more SDM research should be fulfilled in the future to integrate relevant bio-ecological data and climatic/environmental data, which will help us to elucidate the mechanisms of habitat distribution (associated with climate change) of biologically and socioeconomically key seaweed species.

5. Conclusions

This study employed the MaxEnt approach to predict the present and future habitat suitability for *N. haitanensis* and *N. yezoensis*. Additionally, the phylogeographic pattern of the species was profiled based on chloroplast *rbc*L sequences. Except for the main distribution in their native habitats in Northwest Pacific, the models predicted their current potential distribution in other regions, especially in North America. Northward and offshore expansion were identified for both species under the three scenarios in 2050 s. Both species had overall low haplotype and nucleotide diversity while higher divergence was identified at the convergence of the major ocean currents in Northwest Pacific. The geographic distribution centers of *N. yezoensis* and *N. haitanensis* were generally distributed where the genetic diversity hotspots were. The results revealed the potential of *N. yezoensis* and *N. haitanensis* to adapt to future climate change. Laver aquaculture may benefit from global warming. These findings would contribute to conservation and sustainable utilization of *N. haitanensis* and *N. yezoensis* under global climate change.

CRediT authorship contribution statement

Wenyuan Zhou: Writing – original draft, Investigation, Visualization. **Baoxian Li:** Writing – original draft, Investigation. **Hui Xu:** Methodology, Visualization, Validation. **Zhourui Liang:** Methodology, Validation. **Xiaoping Lu:** Methodology. **Lien Yang:** Methodology, Validation. **Wenjun Wang:** Supervision, Project administration, Conceptualization, Writing – review & editing.

Declaration of Competing Interest

The authors declare that they have no known competing financial interests or personal relationships that could have appeared to influence the work reported in this paper.

Data availability

The data that has been used is confidential.

Acknowledgement

This work was supported by the National Key R&D Program of China 'Scientific and Technological Innovation of Blue Granary' (2018YFD0901504), the earmarked fund for CARS-50, Shandong Province Key Research and Development Program (2022LZGC004, 2021LZGC004), the Central Public-interest Scientific Institution Basal Research Fund (2020TD27).

Appendix A. Supplementary data

Supplementary data to this article can be found online at https://doi.org/10.1016/j.ecolind.2023.110219.

References

Ai, Y., Sun, J., Wang, N., Gao, M., Li, X., 2022. Effects of high temperature stress on conchospore germination and early seedling development of *Pyropia haitanensis*. Aquac. Res. 53, 3975–3983. https://doi.org/10.1111/are.15900.

Akaike, H., 1998. Information Theory and an Extension of the Maximum Likelihood Principle, in Selected Papers of Hirotugu Akaike, ed. Parzen, E., Tanabe, K., Kitagawa, G. (New York, NY: Springer New York), 199-213.

Alahuhta, J., Heino, J., Luoto, M., 2011. Climate change and the future distributions of aquatic macrophytes across boreal catchments. J. Biogeogr. 38, 383–393. https://doi.org/10.1111/j.1365-2699.2010.02412.x.

Allcock, A.L., Strugnell, J.M., 2012. Southern Ocean diversity: new paradigms from molecular ecology. Trends Ecol. Evol. 27, 520–528. https://doi.org/10.1016/j.tree.2012.05.009.

Anon., 2017. Inventaire national du Patrimoine naturel. Website. Paris: Muséum National d'Histoire Naturelle. Accessed September 2017.

Araújo, M.B., Pearson, R.G., Thuiller, W., Erhard, M., 2005. Validation of species–climate impact models under climate change. Glob Chang Biol. 11, 1504–1513. https://doi.org/10.1111/j.1365-2486.2005.01000.x.

Assis, J., Tyberghein, L., Bosh, S., Verbruggen, H., Serrão, E.A., De Clerck, O., 2017. Bio-ORACLE v2.0: Extending marine data layers for bioclimatic modelling. Global Ecol. Biogeogr.

Austin, M.P., Van Niel, K.P., 2011. Improving species distribution models for climate change studies: variable selection and scale. J. Biogeogr. 38, 1–8. https://doi.org/10.1111/j.1365-2699.2010.02416.x.

Avise, J.C., 2009. Phylogeography: retrospect and prospect. J. Biogeogr. 36, 3–15. https://doi.org/10.1111/j.1365-2699.2008.02032.x.

Avise, J.C., 2000. Phylogeography: The History and Formation of Species. Harvard University Press, Cambridge, Massachusetts, London, England. P vii, 3.

Bieler, R., Granados-Cifuentes, C., Rawlings, T.A., Sierwald, P., Collins, T.M., 2017. Non-native molluscan colonizers on deliberately placed shipwrecks in the Florida Keys, with description of a new species of potentially invasive worm-snail (Gastropoda: Vermetidae). Peer J. 5, e3158.

Blouin, N.A., Brodie, J.A., Grossman, A.C., Xu, P., Brawley, S.H., 2011. *Porphyra*: a marine crop shaped by stress. Trends Plant Sci. 16, 29–37. https://doi.org/10.1016/j.tplants.2010.10.004.

Boakes, E.H., McGowan, P.J., Fuller, R.A., Ding, C.Q., Clark, N.E., Mace, G.M., 2010. Distorted views of biodiversity: spatial and temporal bias in species occurrence data. PLoS Biol. 8, e1000385.

Bombin, S., Wysor, B., Lopez-Bautista, J.M., 2021. Assessment of littoral algal diversity from the northern Gulf of Mexico using environmental DNA metabarcoding. J. Appl. Phycol. 57, 269–278. https://doi.org/10.1111/jpy.13087.

Bopp, L., Resplandy, L., Orr, J.C., Doney, S.C., Dunne, J.P., Gehlen, M., et al., 2013. Multiple stressors of ocean ecosystems in the 21st century: projections with CMIP5 models. Biogeosciences 10, 6225–6245. https://doi.org/10.5194/bg-10-6225-2013.

Breeman, A.M., 1988. Relative importance of temperature and other factors in determining geographic boundaries of seaweeds: Experimental and phenological evidence. Helgoländer Meeresuntersuchungen 42, 199–241. https://doi.org/10.1007/BF02366043.

Briggs, J.C., 2003. Marine centres of origin as evolutionary engines. J. Biogeogr. 30, 1–18. https://doi.org/10.1046/j.1365-2699.2003.00810.x.

Brodie, J., Wilbraham, J., Pottas, J., Guiry, M., 2015. A revised check-list of the seaweeds of Britain. J. Mar. Biolog. Assoc. U.K. 96, 1005–1029. https://doi.org/10.1017/S0025315415001484.

Brown, J.L., Bennett, J.R., French, C.M., 2017. SDMtoolbox 2.0: the next generation Python-based GIS toolkit for landscape genetic, biogeographic and species distribution model analyses. Peer J. 5, e4095.

Caldeira, K., Wickett, M.E., 2003. Oceanography: anthropogenic carbon and ocean pH. Nature 425, 365. https://doi.org/10.1038/425365a.

Cao, M., Xu, K., Yu, X., Bi, G., Kong, F., Sun, P., Tang, X., Du, G., Ge, Y., Wang, D., Mao, Y., 2020. A chromosome-level genome assembly of *Pyropia haitanensis* (Bangiales, Rhodophyta). Mol. Ecol. Resour. 20, 216–227. https://doi.org/10.1111/1755-0998.13102.

Carss, D.N., Elston, D.A., 2003. Patterns of association between algae, fishes and grey herons Ardea cinerea in the rocky littoral zone of a Scottish sea loch. Estuar. Coast. Shelf Sci. 58, 265–277. https://doi.org/10.1016/S0272-7714(03)00079-9.

Cheung, W.W.L., Lam, V.W.Y., Sarmiento, J.L., Kearney, K., Watson, R., Pauly, D., 2009. Projecting global marine biodiversity impacts under climate change scenarios. Fish Fish (Oxf.) 10, 235–251. https://doi.org/10.1111/j.1467-2979.2008.00315.x.

Davis, M., Shaw, R., 2001. Range shifts and adaptive responses to quaternary climate change. Science (New York, N.Y.). 292, 673–679. https://doi.org/10.1126/science.292.5517.673.

Davison, I.R., Pearson, G.A., 1996. Stress tolerance in intertidal seaweeds. J. Appl. Phycol. 32, 197–211. https://doi.org/10.1111/j.0022-3646.1996.00197.x.

Doney, S.C., Ruckelshaus, M., Emmett Duffy, J., Barry, J.P., Chan, F., English, C.A., et al., 2011. Climate change impacts on marine ecosystems. Ann. Rev. Mar. Sci. 4, 11–37. https://doi.org/10.1146/annurev-marine-041911-111611.

Dulvy, N.K., Rogers, S.I., Jennings, S., Stelzenmüller, V., Dye, S.R., Skjoldal, H.R., 2008. Climate change and deepening of the North Sea fish assemblage: a biotic indicator of warming seas. J. Appl. Ecol. 45, 1029–1039. https://doi.org/10.1111/j.1365-2664.2008.01488.x.

Elith, J., Graham, C.H., Anderson, R.P., Dudík, M., Ferrier, S., Guisan, A., et al., 2006. Novel methods improve prediction of species' distributions from occurrence data. Ecography 29, 129–151. https://doi.org/10.1111/j.2006.0906-7590.04596.x.

Elith, J., Kearney, M., Phillips, S., 2010. The art of modelling range-shifting species. Ecol. EvolMethods Ecol. Evol. 1, 330–342. https://doi.org/10.1111/j.2041-210X.2010.00036.x.

Evans, M.E.K., Merow, C., Record, S., McMahon, S.M., Enquist, B.J., 2016. Towards Process-based Range Modeling of Many Species. Trends Ecol. Evol. 31, 860–871. https://doi.org/10.1016/j.tree.2016.08.005.

Fielding, A.H., Bell, J.F.J.E.C., 1997. A review of methods for the assessment of prediction errors in conservation presence/absence models. Environ. Conserv. 24, 38–49. https://doi.org/10.1017/s0376892997000088.

Flukes, E.B., Wright, J.T., Johnson, C.R., 2015. Phenotypic plasticity and biogeographic variation in physiology of habitat-forming seaweed: response to temperature and nitrate. J. Appl. Phycol. 51, 896–909. https://doi.org/10.1111/jpy.12330.

Franco, J.N., Tuya, F., Bertocci, I., Rodríguez, L., Martínez, B., Sousa-Pinto, I., et al., 2018. The 'golden kelp' *Laminaria ochroleuca* under global change: Integrating multiple eco-physiological responses with species distribution models. J. Ecol. 106, 47–58. https://doi.org/10.1111/1365-2745.12810.

Gebrewahid, Y., Abrehe, S., Meresa, E., Eyasu, G., Abay, K., Gebreab, G., et al., 2020. Current and future predicting potential areas of *Oxytenanthera abyssinica* (A. Richard) using MaxEnt model under climate change in Northern Ethiopia. Ecol. Process. 9, 6. https://doi.org/10.1186/s13717-019-0210-8.

Graham, C.H., Ferrier, S., Huettman, F., Moritz, C., Peterson, A.T., 2004. New developments in museum-based informatics and applications in biodiversity analysis. Trends Ecol. Evol. 19, 497–503. https://doi.org/10.1016/j.tree.2004.07.006.

Graham, M.H., Kinlan, B.P., Druehl, L.D., Garske, L.E., Banks, S., 2007. Deep-water kelp refugia as potential hotspots of tropical marine diversity and productivity. Proc. Natl. Acad. Sci. 104, 16576–16580. https://doi.org/10.1073/pnas.0704778104.

Grant, W.A.S., Bowen, B.W., 1998. Shallow population histories in deep evolutionary lineages of marine fishes: Insights from sardines and anchovies and lessons for conservation. J. Hered. 89 (5), 415–426. https://doi.org/10.1093/jhered/89.5.415.

Gruber, N., 2011. Warming up, turning sour, losing breath: ocean biogeochemistry under global change. Philosophical transactions. Philos. Trans. A Math. Phys. Eng. Sci. 369, 1980–1996. https://doi.org/10.1098/rsta.2011.0003.

Guillemin, M.L., Dubrasquet, H., Reyes, J., Valero, M., 2018. Comparative phylogeography of six red algae along the Antarctic peninsula: extreme genetic depletion linked to historical bottlenecks and recent expansion. Polar Biol. 41, 827–837. https://doi.org/10.1007/s00300-017-2244-7.

Guinotte, J.M., Fabry, V.J., 2008. Ocean acidification and its potential effects on marine ecosystems. Ann. N. Y. Acad. Sci. 1134, 320–342. https://doi.org/10.1196/annals.1439.013.

Harley, C.D., Randall, H.A., Hultgren, K.M., Miner, B.G., Sorte, C.J., Thornber, C.S., et al., 2006. The impacts of climate change in coastal marine systems. Ecol. Lett. 9, 228–241. https://doi.org/10.1111/j.1461-0248.2005.00871.x.

Hirabayashi, K., Murch, S.J., Erland, L.A.E., 2022. Predicted impacts of climate change on wild and commercial berry habitats will have food security, conservation and agricultural implications. Sci. Total Environ. 845, 157341 https://doi.org/10.1016/j.scitotenv.2022.157341.

Hu, Z.M., Li, J.J., Sun, Z.M., Gao, X., Yao, J.T., Choi, H.G., Endo, H., Duan, D.L., 2017. Hidden diversity and phylogeographic history provide conservation insights for the edible seaweed *Sargassum fusiforme* in the northwest Pacific. Evol. Appl. 10, 366–378.

Jueterbock, A., Tyberghein, L., Verbruggen, H., Coyer, J.A., Olsen, J.L., Hoarau, G., 2013. Climate change impact on seaweed meadow distribution in the North Atlantic rocky intertidal. Ecol. Evol. 3, 1356–1373. https://doi.org/10.1002/ece3.541.

Jueterbock, A., Smolina, I., Coyer, J.A., Hoarau, G., 2016. The fate of the Arctic seaweed Fucus distichus under climate change: an ecological niche modeling approach. Ecol. Evol. 6, 1712–1724. https://doi.org/10.1002/ece3.2001.

Khanum, R., Mumtaz, A., Kumar, S., 2013. Predicting impacts of climate change on medicinal asclepiads of Pakistan using Maxent modeling. Acta Oecol. 49, 23–31. https://doi.org/10.1016/j.actao.2013.02.007.

Kim, S.M., Choi, H.G., Hwang, M.S., Kim, H.S., 2018. Biogeographic pattern of four endemic *Pyropia* from the east coast of Korea, including a new species *Pyropia retorta* (Bangiaceae, Rhodophyta). Algae 33, 55–68. https://doi.org/10.4490/algae.2018.33.2.26.

Kim, H.S., Choi, H.G., Hwang, M.S., Jeon, Y.J., Yarish, C., Kim, J.K., 2022. Concise review of the genus *Neopyropia* (Rhodophyta: Bangiales). J. Appl. Phycol. 34, 1805–1824. https://doi.org/10.1007/s10811-022-02776-1.

Koh, Y.H., Kim, M.S., 2020. Genetic diversity and distribution pattern of economic seaweeds *Pyropia yezoensis* and *Py. suborbiculata* (Bangiales, Rhodophyta) in the northwest Pacific. J. Appl. Phycol. 32, 2495–2504. https://doi.org/10.1007/s10811-019-01984-6.

Kornmann, P., Sahling, P.H., 1991. The *Porphyra* species of Helgoland (Bangiales, Rhodophyta). Helgoländer Meeresuntersuchungen 45, 1–38. https://doi.org/10.1007/BF02365634.

Laeseke, P., Martínez, B., Mansilla, A., Bischof, K., 2020. Future range dynamics of the red alga *Capreolia implexa* in native and invaded regions: contrasting predictions from species distribution models versus physiological knowledge. Biol. Invasions. 22, 1339–1352. https://doi.org/10.1007/s10530-019-02186-4.

Li, X.L., Wang, W.J., Liu, F.L., Liang, Z.R., Sun, X.T., Yao, H.Q., Wang, F.J., 2018. Periodical drying or no drying during aquaculture affects the desiccation tolerance of a sublittoral *Pyropia yezoensis* strain. J. Appl. Phycol. 30 (1), 697–705. https://doi.org/10.1007/s10811-017-1227-y.

Li, G.L., Wang, W.J., Li, B.X., Yao, H.Q., Sun, X., Liang, Z.R., et al., 2021. Potential geographic distribution of *Costaria costata* in China based on MaxEnt Model and ArcGIS. J. Fish. Sci. Chn. 28 (12), 1588–1601. https://doi.org/10.12264/JFSC2021-0108.

Li, M., Xu, K., Tang, X., Zhang, L., Xu, Y., Wang, W., Ji, D., Chen, C., Xie, C., 2021. Effects of ocean acidification on the light and temperature adaptations of commercial seaweed *Pyropia haitanensis*. J Oceanogr. 40 (3), 388–394. https://doi.org/10.3969/J.ISSN.2095-4972.2021.03.003.

Liang, Z.R., Wang, W.J., Liu, L.L., Li, G.L., 2022a. The influence of ecological factors on the contents of nutritional components and minerals in laver based on open sea culture system. J. Mar. Sci. Eng. 10, 864. https://doi.org/10.3390/jmse10070864.

Liang, Z.R., Wang, W.J., Liu, L.L., Li, G.L., Xia, B., 2022b. Influence of commercial-scale seaweed cultivation on water quality: a case study in a typical laver culture area of the Yellow Sea. North China. J. Mar. Sci. Eng. 10, 681. https://doi.org/10.3390/jmse10050681.

Ma, S., Liu, D., Tian, Y., Fu, C., Li, J., Ju, P., et al., 2021. Critical transitions and ecological resilience of large marine ecosystems in the Northwestern Pacific in response to global warming. Glob Chang Biol. 27, 5310–5328. https://doi.org/10.1111/gcb.15815.

Mac Nally, R., 2000. Regression and model-building in conservation biology, biogeography and ecology: The distinction between – and reconciliation of – 'predictive' and 'explanatory' models. Biodivers. Conserv. 9, 655–671. https://doi.org/10.1023/A:1008985925162.

Marc, R., Xavier, T., 2020. Phylogeography and the Description of Geographic Patterns in Invasion Genomics. Front. Ecol. Evol. 8, 595711 https://doi.org/10.3389/fevo.2020.595711.

Marien, Michael., 2011. Climate Stabilization Targets: Emissions, Concentrations, and Impacts over Decades to Millennia. World Future Review. The National Academies Press, Washington, DC.

Martín-García, L., Herrera, R., Moro-Abad, L., Sangil, C., Barquín-Diez, J., 2014. Predicting the potential habitat of the harmful cyanobacteria *Lyngbya majuscula* in the Canary Islands (Spain). Harmful Algae 34, 76–86. https://doi.org/10.1016/j.hal.2014.02.008.

Mineur, F., Arenas, F., Assis, J., Davies, A.J., Engelen, A.H., Fernandes, F., et al., 2015. European seaweeds under pressure: Consequences for communities and ecosystem functioning. J. Sea Res. 98, 91–108. https://doi.org/10.1016/j.seares.2014.11.004.

Mueter, F.J., Litzow, M.A., 2008. Sea ice retreat alters the biogeography of the Bering Sea continental shelf. Ecol. Appl. 18, 309–320. https://doi.org/10.1890/07-0564.1.

Murcia, S., Riul, P., Mendez, F., Rodriguez, J.P., Rosenfeld, S., Ojeda, J., et al., 2020. Predicting distributional shifts of commercially important seaweed species in the Subantarctic tip of South America under future environmental changes. J. Appl. Phycol. 32, 2105–2114. https://doi.org/10.1007/s10811-020-02084-6.

Neefus, C., Mathieson, A., Bray, T., Yarish, C., 2008. The distribution, morphology, and ecology of three introduced asiatic species of *Porphyra* (Bangiales, Rhodophyta) in the northwestern Atlantic. J. Appl. Phycol. 44, 1399–1414. https://doi.org/10.1111/j.1529-8817.2008.00607.x.

Olischläger, M., Bartsch, I., Gutow, L., Wiencke, C., 2012. Effects of ocean acidification on different life-cycle stages of the kelp *Laminaria hyperborea* (Phaeophyceae). Botanica Marina 55, 511–525. https://doi.org/10.1515/bot-2012-0163.

Parmesan, C., 2006. Ecological and evolutionary responses to recent climate change. Annu. Rev. Ecol. Evol. Syst. 37, 637–669. https://doi.org/10.1146/annurev.ecolsys.37.091305.110100.

Parmesan, C., Ryrholm, N., Stefanescu, C., Hill, J.K., Thomas, C.D., Descimon, H., et al., 1999. Poleward shifts in geographical ranges of butterfly species associated with regional warming. Nature 399, 579–583. https://doi.org/10.1038/21181.

Parmesan, C., Yohe, G., 2003. A globally coherent fingerprint of climate change impacts across natural systems. Nature 421, 37–42. https://doi.org/10.1038/nature01286.
Peterson, A.T., Ortega-Huerta, M.A., Bartley, J., Sánchez-Cordero, V., Soberón, J., Buddemeier, R.H., et al., 2002. Future projections for *Mexican faunas* under global climate change scenarios. Nature 416, 626–629. https://doi.org/10.1038/416626a.
Petrocelli, A., Cecere, E., 2019. A 20-year update on the state of seaweed resources in Italy. Botanica Marina 62, 249–264. https://doi.org/10.1515/bot-2018-0072.
Phillips, S.J., Dudík, M., 2008. Modeling of species distributions with Maxent: new extensions and a comprehensive evaluation. Ecography 31, 161–175. https://doi.org/10.1111/j.0906-7590.2008.5203.x.
Phillips, S.J., Dudík, M., Elith, J., Graham, C.H., Lehmann, A., Leathwick, J., Ferrier, S., 2009. Sample selection bias and presence-only distribution models: implications for background and pseudo-absence data. Ecol. Appl. 19, 181–197. https://doi.org/10.1890/07-2153.1.
Popova, E., Yool, A., Byfield, V., Cochrane, K., Coward, A.C., Salim, S.S., et al., 2016. From global to regional and back again: common climate stressors of marine ecosystems relevant for adaptation across five ocean warming hotspots. Glob Chang Biol. 22, 2038–2053. https://doi.org/10.1111/gcb.13247.
Sano, F., Ikeura, A., Takasugi, A., Niwa, K., 2021. First record of *Neoporphyra haitanensis* (T.J.Chang & B.F.Zheng) J. Brodie & L.-E.Yang (Bangiales, Rhodophyta) from Shikinejima Island and Hachijojima Island of the Izu Islands, southern central Japan. Phycol. Res. 69, 258–265. https://doi.org/10.1111/pre.12466.
Sfriso, A., Buosi, A., Wolf, M.A., Sfriso, A.A., 2019. Invasion of alien macroalgae in the Venice Lagoon, a pest or a resource? Aquat. 15 (2), 245–270. https://doi.org/10.3391/ai.2020.15.2.03.
Sheehy, D.J., Vik, S.F., 2010. The role of constructed reefs in non-indigenous species introductions and range expansions. Ecol. Eng. 36, 1–11. https://doi.org/10.1016/j.ecoleng.2009.09.012.
Song, W.H., Li, J.J., 2023. The effects of intraspecific variation on forecasts of species range shifts under climate change. Sci. Total Environ. 857 (Part 2), 159513 https://doi.org/10.1016/j.scitotenv.2022.159513.
Sprung, M. J., Nguyen, L. X., Riley, D., Zhou, S., Lawson, A., 2018. National Transportation Statistics 2018. U.S. Department of Transportation, Bureau of Transportation Statistics, Washington, DC, pp 1–24.
Steen, V.A., Tingley, M.W., Paton, P.W.C., Elphick, C.S., 2021. Spatial thinning and class balancing: Key choices lead to variation in the performance of species distribution models with citizen science data. Methods Ecol. Evol. 12, 216–226. https://doi.org/10.1111/2041-210X.13525.
Tanaka, K., Taino, S., Haraguchi, H., Prendergast, G., Kiraoka, M., 2012. Warming off southwestern Japan linked to distributional shifts of subtidal canopy-forming seaweeds. Ecol. Evol. 2, 2854–2865. https://doi.org/10.1002/ece3.391.
Thuiller, W., Richardson, D.M., PyŠEk, P., Midgley, G.F., Hughes, G.O., Rouget, M., 2005. Niche-based modelling as a tool for predicting the risk of alien plant invasions at a global scale. Glob. Chang Biol. 11, 2234–2250. https://doi.org/10.1111/j.1365-2486.2005.001018.x.
Tyberghein, L., Verbruggen, H., Pauly, K., Troupin, C., Mineur, F., De Clerck, O., 2012. Bio-ORACLE: a global environmental dataset for marine species distribution modelling. Glob. Ecol. Biogeogr. 21, 272–281. https://doi.org/10.1111/j.1466-8238.2011.00656.x.
van Vuuren, D.P., Edmonds, J., Kainuma, M., Riahi, K., Thomson, A., Hibbard, K., et al., 2011. The representative concentration pathways: an overview. Clim Change 109, 5. https://doi.org/10.1007/s10584-011-0148-z.
Vanderwal, J., Murphy, H., Kutt, A., Perkins, G., Bateman, B., Perry, J., et al., 2013. Focus on poleward shifts in species' distribution underestimates the fingerprint of climate change. Nat. Clim. Change. 3, 239–243. https://doi.org/10.1038/NCLIMATE1688.
Verbruggen, H., Tyberghein, L., Belton, G.S., Mineur, F., Jueterbock, A., Hoarau, G., et al., 2013. Improving transferability of introduced species' distribution models: new tools to forecast the spread of a highly invasive seaweed. PloS One 8, e68337.
Wang, W.J., Sun, X.T., Liu, F.L., Liang, Z.R., Zhang, J.H., Wang, F.J., 2016. Effect of abiotic stress on the gameophyte of *Pyropia katadae* var. *hemiphylla* (Bangiales, Rhodophyta). J. Appl. Phycol. 28 (1), 469–479. https://doi.org/10.1007/s10811-015-0579-4.
Wernberg, T., Russell, B.D., Moore, P.J., Ling, S.D., Smale, D.A., Campbell, A., et al., 2011. Impacts of climate change in a global hotspot for temperate marine biodiversity and ocean warming. J. Exp. Mar. Biol. Ecol. 400, 7–16. https://doi.org/10.1016/j.jembe.2011.02.021.
West, A., Mathieson, A., Klein, A., Neefus, C., Bray, T., 2005. Molecular ecological studies of New England species of *Porphyra* (Rhodophyta, Bangiales). Nova Hedwigia. 80, 1–24. https://doi.org/10.1127/0029-5035/2005/0080-0001.
Wiltshire, K.H., Tanner, J.E., 2020. Comparing maximum entropy modelling methods to inform aquaculture site selection for novel seaweed species. Ecol Modell. 429, 109071 https://doi.org/10.1016/j.ecolmodel.2020.109071.
Wisz, M.S., Hijmans, R.J., Li, J., Peterson, A.T., Graham, C.H., Guisan, A., 2008. Effects of sample size on the performance of species distribution models. Divers. Distrib. 14, 763–773. https://doi.org/10.1111/j.1472-4642.2008.00482.x.
Wynne, M., 2008. A checklist of benthic marine algae of the coast of texas. Gulf Mex. Sci. 26, 64–87. https://doi.org/10.18785/goms.2601.07.
Xian, Y., Lu, Y., Liu, G., 2022. Is climate change threatening or beneficial to the habitat distribution of global pangolin species? Evidence from species distribution modeling. Sci. Total Environ. 811, 151385 https://doi.org/10.1016/j.scitotenv.2021.151385.
Xu, K., Tang, X., Wang, L., Yu, X., Sun, P., Mao, Y., 2018. Divergence time, historical biogeography and evolutionary rate estimation of the order Bangiales (Rhodophyta) inferred from multilocus data. Chin. J. Oceanol. Limnol. 36, 870–881. https://doi.org/10.1007/s00343-018-7054-4.
Yang, L., Deng, Y., Xu, G., Russell, S., Lu, Q., Brodie, J., 2020. Redefning *Pyropia* (Bangiales, Rhodophyta): four new genera, resurrection of *Porphyrella* and description of *Calidia pseudolobata* sp. nov. from China. J. Appl. Phycol. 56, 862–879. https://doi.org/10.1111/jpy.12992.
Yang, X.Q., Kushwaha, S.P.S., Saran, S., Xu, J., Roy, P.S., 2013. Maxent modeling for predicting the potential distribution of medicinal plant, *Justicia adhatoda* L. in Lesser Himalayan foothills. Ecol. Eng. 51, 83–87. https://doi.org/10.1016/j.ecoleng.2012.12.004.
Yang, L.E., Lu, Q.Q., Brodie, J., 2017. A review of the bladed Bangiales (Rhodophyta) in China: history, culture and taxonomy. European J. Appl. Phycol. 52 (3), 251–263. https://doi.org/10.1080/09670262.2017.1309689.
Yang, L.E., Zhou, W., Hu, C.M., Deng, Y.Y., Xu, G.P., Zhang, T., Russell, S., Zhu, J.Y., Lu, Q.Q., Brodie, J., 2018. A molecular phylogeny of the bladed Bangiales (Rhodophyta) in China provides insights into biodiversity and biogeography of the genus Pyropia. Mol. Phylogenet. Evol. 120, 94–102. https://doi.org/10.1016/j.ympev.2017.11.009.
Zhu, G., Qiao, H., 2016. Effect of the Maxent model's complexity on the prediction of species potential distributions. Biodiversity Sci. 24, 1189–1196. https://doi.org/10.17520/biods.2016265.